Z. Phys. C – Particles and Fields 33, 351–357 (1987)

Zeitschrift für Physik C Particles and Fields

Jet Production in Photon-Photon Interactions

PLUTO Collaboration

Ch. Berger, H. Genzel, W. Lackas, J. Pielorz[a], F. Raupach, W. Wagner[b]
I. Physikalisches Institut der RWTH Aachen[c], D-5100 Aachen, Federal Republic of Germany

A. Klovning, E. Lillestöl,
University of Bergen[d], N-5014 Bergen, Norway

J. Bürger, L. Criegee, A. Deuter, F. Ferrarotto[e], G. Franke, M. Gaspero[e], Ch. Gerke, G. Knies, B. Lewendel, J. Meyer, U. Michelson, K.H. Pape, B. Stella[e], U. Timm, G.G. Winter, M. Zachara[f], W. Zimmermann
Deutsches Elektronen-Synchrotron (DESY), D-2000 Hamburg, Federal Republic of Germany

P.J. Bussey, S.L. Cartwright[g], J.B. Dainton[h], D. Hendry, B.T. King[h], C. Raine, J.M. Scarr, I.O. Skillicorn, K.M. Smith, J.C. Thomson[i]
University of Glasgow[j], Glasgow, UK

O. Achterberg, V. Blobel, D. Burkart, K. Diehlmann, M. Feindt, H. Kapitza[k], B. Koppitz, M. Krüger[l], M. Poppe, H. Spitzer, R. van Staa
II. Institut für Experimentalphysik der Universität, D-2000 Hamburg[c], Federal Republic of Germany

C.Y. Chang, R.G. Glasser, R.G. Kellogg, S.J. Maxfield[m], R.O. Polvado, B. Sechi-Zorn[a], J.A. Skard, A. Skuja, A.J. Tylka[n], G.E. Welch, G.T. Zorn
University of Maryland[o], College Park, MD 20742, USA

F. Almeida[p], A. Bäcker, F. Barreiro[q], S. Brandt, K. Derikum[r], C. Grupen, H.J. Meyer, H. Müller, B. Neumann, M. Rost, K. Stupperich, G. Zech
Universität-Gesamthochschule Siegen[c], D-5900 Siegen, Federal Republic of Germany

G. Alexander, G. Bella, Y. Gnat, J. Grunhaus
University of Tel-Aviv[s], Israel

H. Junge, K. Kraski, C. Maxeiner, H. Maxeiner, H. Meyer, D. Schmidt
Universität-Gesamthochschule Wuppertal[c], D-5600 Wuppertal, Federal Republic of Germany

Received 4 September 1986

[a] Deceased
[b] Now at University of California at Davis, Davis, Ca., USA
[c] Supported by the BMFT, Federal Republic of Germany
[d] Partially supported by the Norwegian Council for Science and the Humanities
[e] Rome University, partially supported by I.N.F.N., Sezione di Roma, Italy
[f] Institute of Nuclear Physics, Cracow, Poland
[g] Now at Rutherford Appleton Laboratory, Chilton, UK
[h] Now at University of Liverpool, Liverpool, UK
[i] Now at University of Strathclyde, Glasgow, UK
[j] Supported by the U.K. Science and Engineering Research Council
[k] Now at Carleton University, Ottawa, Ontario, Canada
[l] Now at Universität Karlsruhe, Federal Republic of Germany
[m] Now at University of Massachussetts, Amherst, Mass., USA
[n] Now at Naval Research Laboratory, Washington, USA
[o] Partially supported by the Department of Energy, USA
[p] On leave of absence from Inst. de Fisica, Universidad Federal do Rio de Janeiro, Brasil
[q] On leave of absence at Universidad Autonoma de Madrid, Spain
[r] Now at BESSY, D-1000 Berlin, Federal Republic of Germany
[s] Partially supported by the Israeli Academy of Sciences and Humanities – Basic Research Foundation

Abstract. We present results on jet production in $\gamma\gamma$ interactions where both photons are quasi-real. The invariant masses of the hadronic system are limited to the range $4 \leqq W_{vis} \leqq 12$ GeV/c^2. The data approach the Quark-Parton-Model (QPM) expectation at the highest p_T^{jet} values ($\geqq 4$ GeV/c). Jet production at low p_T ($\leqq 1$ GeV/c) can be described by a Vector Dominance derived model. The data also have a component with no apparent jet structure in the range, $1.0 \leqq p_T^{jet} \leqq 4.0$ GeV/c which can be described by phase space or by models of the QCD hard scattering processes $\gamma\gamma \to q\bar{q}g$ and $\gamma\gamma \to q\bar{q}q\bar{q}$.

Introduction

The production of two-jet events in $\gamma\gamma$ interactions [1] has been studied by the JADE [2], TASSO [2] and PLUTO [3] collaborations. These studies have shown that for virtual photons the cross-section for the production of jets with high transverse momentum, p_T^{jet}, relative to the $\gamma\gamma$ axis approaches that predicted by the quark parton model (QPM) (Fig. 1a) as p_T^{jet} increases. In contrast, for low p_T^{jet}, the data are well described by models based on vector dominance (VDM) in which the photons interact via their hadronic components, (Fig. 1b). For the case of quasi-real $\gamma\gamma$ interactions the TASSO collaboration have reported on the production of charged hadrons in the range $1.5 \leqq p_T \leqq 3.0$ GeV/c where they observe an excess of hadrons over the predictions of the QPM by a factor of four. This observation has been confirmed by the PLUTO collaboration [3] who have shown however that the excess is not present when events with high p_T^{jet} are selected and that the cross-section for high p_T^{jet} is in agreement with the QPM expectation.

Higher order QCD calculations predict the production of multijet events in $\gamma\gamma$ interactions [4] (Fig. 1c, d) in addition to the two-jet topology. In this paper we report on the results of an analysis of events of the type $e^+e^- \to e^+e^-$ + hadrons where the scattered electrons are anti-tagged and consequently the interacting photons are constrained to be quasi-real. We present an analysis of the topology of these $\gamma\gamma$ events and evidence for the presence of higher order QCD processes.

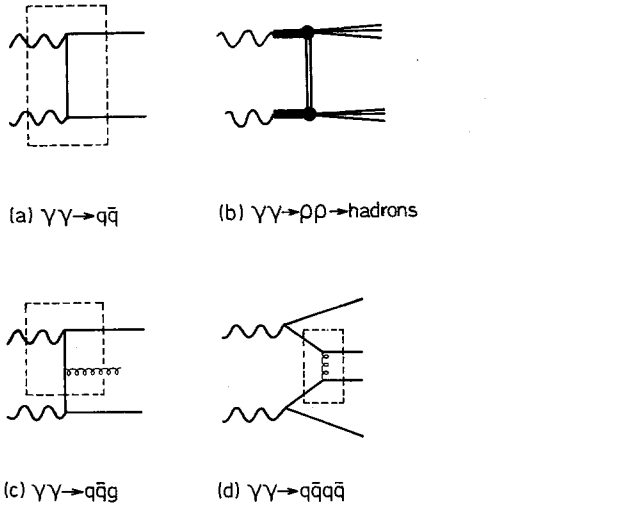

Fig. 1. a The pointlike QPM interaction. **b** The VDM interaction. **c** $\gamma\gamma \to q\bar{q}g$. **d** $\gamma\gamma \to q\bar{q}q\bar{q}$. The hard scattering subprocess is indicated by the dashed line

The Pluto Detector

The data were obtained with the PLUTO detector at the storage ring PETRA, at an e^+e^- centre of mass energy of 34.7 GeV. The deails of the PLUTO detector have been described in previous publications [3, 5]. In the angular region $25 \leqq \theta \leqq 155°$ detection and momentum measurement of charged particles is performed by a cylindrical central detector, in a solenoidal magnetic field of 1.65 T. In addition, forward spectrometers [6] cover the regions $5 \leqq \theta \leqq 15°$ and $165 \leqq \theta \leqq 175°$ and 85% of full azimuth, providing charged particle detection at small angles to the e^+e^- beams with a momentum resolution of $\sigma_p/p = 3\% \cdot p$ (p in GeV/c). The barrel and endcap shower counters which cover 96% of the full solid angle are used for the detection of photons.

An important feature of the detector for the classification of $\gamma\gamma$ interactions is the presence of electron taggers at small angles to the e^+e^- beam axis. The small angle taggers (SAT) and large angle taggers (LAT) cover the angular regions of $30 \leqq \theta \leqq 55$ mrad and $87 \leqq \theta \leqq 260$ mrad with energy resolutions (σ_E/E with E in GeV) $16.5\%/\sqrt{E}$ and $25\%/\sqrt{E}$ respectively.

Data Selection

If an electron were detected in the SAT or LAT with an energy greater than 8 GeV the event was rejected. This procedure limits the mean Q^2 of the interacting photons to 0.008 GeV^2.

In order to identify jets and also to reduce the large backgrounds in this sample of $\gamma\gamma$ events the following selections were made:

- charged multiplicity $\geqq 4$
- $4 \leqq W_{vis} \leqq 12$ GeV/c^2, where W_{vis} is the observed invariant mass of the hadronic system. The lower limit

is chosen to avoid the region of s-channel resonance production and to ensure sufficient energy for jet formation; the upper limit is required to reduce the background from $e^+e^- \to$ hadrons.

- $|\sum q_i| \leqq 2$, where q denotes the charge of the hadrons in units of e.
- $|\sum \mathbf{p}_{Ti}| \leqq 2$ GeV/c, where $\mathbf{p}_{Ti}$ is the transverse momentum of each particle with respect to the e^+e^- beam axis.
- $|z_0| \leqq 35$ mm, where z_0 is the distance between the interaction vertex and the e^+e^- beam intersection point as measured along the beam axis.

The third and fourth selections reject badly measured events while the last selection suppresses events arising from beam-gas interactions. The residual beam-gas background is estimated from the z_0 sidebands and constitutes 1.5% of the final data sample.

Backgrounds have been calculated by Monte Carlo techniques; the following processes have been considered:

- $e^+e^- \to$ hadrons
- $e^+e^- \to \tau^+\tau^-$
- $e^+e^- \to e^+e^-\tau^+\tau^-$.

The production of tau pairs via one and two photon couplings contributes backgrounds of 0.2 and 0.5% respectively. The most severe background is from the annihilation production of hadrons which contributes 3.1% overall to the data sample [7]. This background is large ($\sim 50\%$) in the regions of high p_T^{jet} ($\geqq 4$ GeV/c) and high thrust ($\geqq 0.8$) and limits the maximum W_{vis}, and hence p_T^{jet}, at which jet production can be studied. The annihilation background has been studied in detail over the full range of invariant masses up to the e^+e^- CM energy; the annihilation Monte Carlo is found to describe the data well in background dominated regions.

From an integrated luminosity of 12 pb^{-1} we obtain a final event sample of 6293 events of which 5.3% are due to background processes. The backgrounds due to beam-gas, annihilation and tau-pair production have been statistically subtracted from the data sample.

Monte Carlo Models

The comparison of theory and experiment is complicated by the limited resolution and acceptances of the detector. We use Monte Carlo techniques to generate events according to the differential $\gamma\gamma$ cross-section predicted by models, and to simulate effects of the detector. To describe hadron production in $\gamma\gamma$ interactions, two classes of model have been used namely:

- jet models which produce a two jet topology. The pointlike QPM process $\gamma\gamma \to q\bar{q}$ and the VDM are of this type. We use the same models that described well the tagged PLUTO data [3].
- multijet models where hadron production is described by higher order QCD processes $\gamma\gamma \to q\bar{q}g$ and $\gamma\gamma \to q\bar{q}q\bar{q}$ or by phase-space.

We now describe the models in more detail.

(a) The Quark Parton and Vector Dominance Models

The event generator for QPM is based on a program due to Vermaseren [8] which simulates the process $e^+e^- \to e^+e^-\mu^+\mu^-$. To generate $\gamma\gamma \to q\bar{q}$ the μ's are replaced by quark-antiquark pairs $u\bar{u}$, $d\bar{d}$, $s\bar{s}$, $c\bar{c}$ with fractional charges and masses of 0.3, 0.3, 0.5 and 1.6 GeV/c^2 respectively. The quarks are fragmented using the standard Feynman-Field [9] scheme. The quarks u, d and s are fragmented using the distribution $dN/dk_T^2 \sim e^{-k_T^2/\sigma^2}$ with $\sigma = 350$ MeV/c, $f(z) = 1 - a + 3a(1-z)^2$ with $a = 0.77$, $P/(P+V) = 0.5$ and a sea quark ratio of $u:d:s = 2:2:1$. The fragmentation of the charm quark follows the prescription in [10].

To simulate the hadronic interaction of the photons we used a Vector Dominance Model with parameters determined from the VDM dominated region of the PLUTO tagged data. Thus the cross-section was taken to be 240 nb and the fragmentation of the two jets follows the Field-Feynmann scheme with $a = 0.45$ and $\sigma = 450$ MeV/c. We use the incoherent sum of QPM and VDM to describe two-jet production and refer to this sum as the two-jet model.

(b) Multi-jet Models

(i) Higher Order QCD Processes. In QCD, higher order processes are predicted to occur in $\gamma\gamma$ interactions with a cross-section of the order of the pointlike $\gamma\gamma \to q\bar{q}$ cross-section [4]. Two of these hard scattering processes, $\gamma\gamma \to q\bar{q}g$ and $\gamma\gamma \to q\bar{q}q\bar{q}$, have been simulated by Monte Carlo. The W-dependence for the $\gamma\gamma$ cross-sections are assumed to be proportional to $1/W^2$. The event simulation is as follows:

$\gamma\gamma \to q\bar{q}g$.

One of the photons is split into a $q\bar{q}$ pair. The quarks are assumed to have a flat x dependence where x is the fractional four-momentum of the photon carried by the quark. The other photon interacts with a quark in a hard scattering process $\gamma q \to qg$, as shown in Fig. 1c. This point-like interaction is assumed to have the same angular distribution in its centre of mass as that in $\gamma\gamma \to q\bar{q}$. Finally the gq system is fragmented in the same way as the $q\bar{q}$ system in the QPM.

$\gamma\gamma \to q\bar{q}q\bar{q}$.

For this channel both of the photons are split into a $q\bar{q}$ pair with a flat x dependence. The hard scattering process $qq \to qq$, see Fig. 1d, is simulated and the quarks are fragmented as for the pointlike $\gamma\gamma \to q\bar{q}$ process.

(ii) Phase-Space. For the low W-values of this data it may not be possible to resolve multijet formation. We therefore consider also phase-space distributions. We have employed two all-pion phase-space models which differ in the W and Q^2 dependence of the $\gamma\gamma$ cross-section. The model called PS1 has the same W and Q^2 dependences for the $\gamma\gamma$ cross-section as the vector dominance derived model ($\sigma^{PS1}(W) \propto W^0$). The second model (PS2) has a QPM like cross-section ($\sigma^{PS2}(W) \propto W^{-2}$). The multiplicity of the pions is taken from e^+e^- annihilation data at comparable centre of mass energies.

These multijet models could be substantially refined by, for example, using an alternative splitting function for the photon and a more accurate description of the hard scattering process. However our motivation for using these models has not been to find an exact description of multijet processes but rather to find out if one model could be distinguished from another at the relatively low $\gamma\gamma$ invariant masses accessible to this experiment [7].

Results

We emphasise that all the distributions shown here include detector effects and therefore cannot be directly compared with theoretical predictions.

The data are analysed in the hadronic centre of mass frame and the jet axis is defined by the thrust axis. In the case of untagged $\gamma\gamma$ events, the photon four-vectors cannot be determined; it is, however, a good approximation to replace the unknown $\gamma\gamma$ axis by the e^+e^- beam axis. The jet transverse momentum, p_T^{jet}, is thus defined with respect to the e^+e^- beam direction.

Jet structure in the data will manifest itself as a limited transverse momentum (k_T) for the hadrons with respect to the jet axis. In contrast, the longitudinal momentum component (k_L) increases with the centre of mass energy. Figure 2 shows the distribution of the mean values of k_T and k_L as a function of the observable hadronic invariant mass W_{vis}. The data are compared with the predictions of the two-jet model and an all pion phase-space model. The band on the Monte-Carlo curve represents ± 1 standard deviations on the statistical uncertainty. Both the k_T limitation and the growth of k_L observed in the data are well described by the jet model demonstrating the dominant two jet structure of the data.

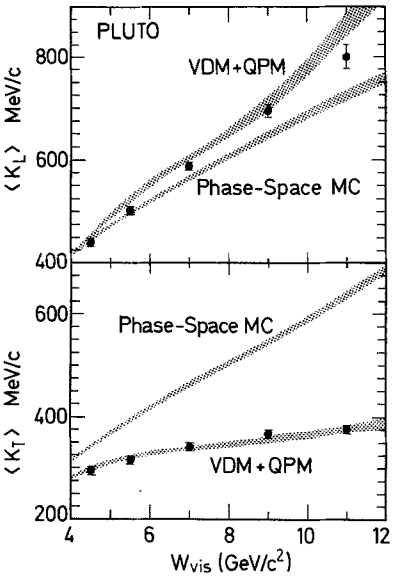

Fig. 2. The average transverse and longitudinal components of momentum for charged particles with respect to the thrust axis in the hadronic centre of mass frame. The data is compared to the incoherent sum of VDM and QPM and to a phase-space model

Having shown the presence of the jet structure in the data, we study the distribution of jet transverse momentum, p_T^{jet}. We compare the data with the pointlike $\gamma\gamma \to q\bar{q}$ process using the quantity:

$$\tilde{R}^{\gamma\gamma}(p_T^{jet}) = \frac{\text{observed number of events at a given } p_T^{jet}}{\text{number of events predicted by QPM at the same } p_T^{jet}}. \quad (1)$$

In Fig. 3 $\tilde{R}^{\gamma\gamma}$ is shown as a function of p_T^{jet} for all the data together with the prediction of the two-jet model. From Fig. 3 we observe:

- At high p_T^{jet} the data approach the QPM expectation from above with $\tilde{R}^{\gamma\gamma} = 1.9 \pm 0.9$ for $p_T^{jet} \geqq 4$ GeV/c.
- Jet production at low p_T is well described by VDM.
- An excess of events over the prediction of the two-jet model is evident in the intermediate p_T^{jet} region of $1.0 \leqq p_T^{jet} \leqq 4.0$ GeV/c. When two-jet events are selected (thrust $\geqq 0.9$), no excess is observed (Fig. 4).

To study the excess of events at intermediate p_T^{jet} we examine the thrust distribution. Figure 5 shows the distribution of thrust together with the prediction of the two-jet model. The two-jet model approaches the observed distribution at high thrust while at low thrust there is an excess of events. To correlate the thrust distribution with the jet transverse momentum we show in Fig. 6 the mean thrust as a function of

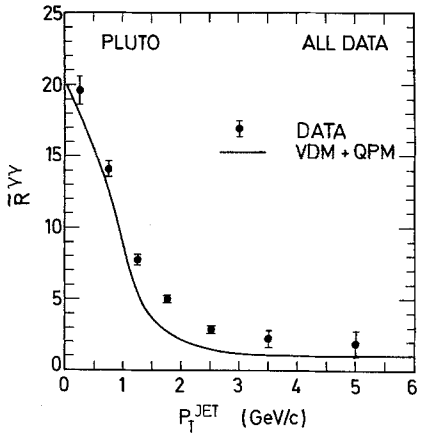

Fig. 3. $\tilde{R}^{\gamma\gamma}$ versus p_T^{jet} for all data. The solid curve represents the predictions from the incoherent sum of VDM and QPM

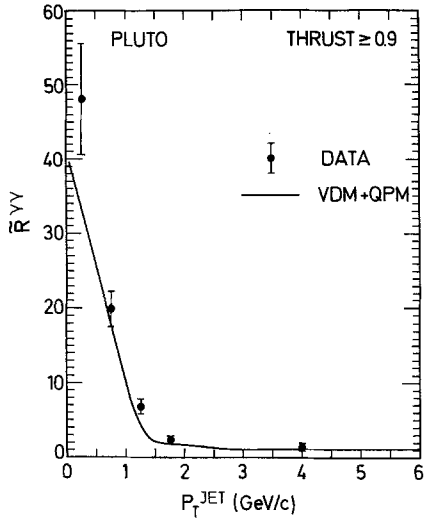

Fig. 4. $\tilde{R}^{\gamma\gamma}$ versus p_T^{jet} for all events with thrust $\geqq 0.9$

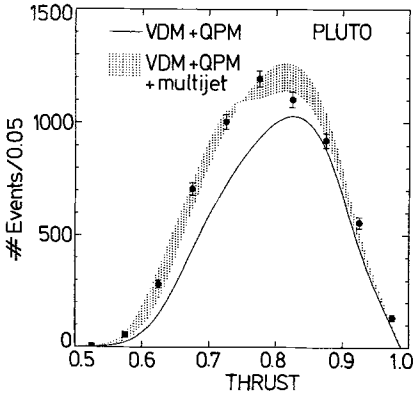

Fig. 5. The thrust distribution. The jet model of the incoherent sum of VDM and QPM is shown by the solid curve. The addition of the multijet models PS2, $q\bar{q}g$ and $q\bar{q}q\bar{q}$ to the two-jet model give a range of thrust distributions shown by the shaded area

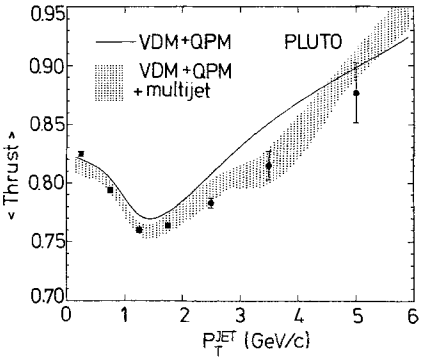

Fig. 6. The mean thrust value as a function of p_T^{jet}. The two-jet model is shown by the solid curve; the sum of the multijet and two-jet models is shown by the shaded area

p_T^{jet}. Evidently the deviation of the mean thrust from that expected for two jets is most marked at intermediate p_T^{jet} values lying between 1.0 and 4.0 GeV/c, i.e. at those p_T^{jet} values where an excess of events is observed in the $\tilde{R}^{\gamma\gamma}(p_T^{jet})$ plot.

The data thus demonstrate the existence of events which have a lower average thrust than two-jet events; we refer to these events as the *low-thrust events*. We take the number of low-thrust events to be equal to the number of data events minus the number of events predicted by the two-jet model. If the two-jet model has the cross-section extrapolated from the PLUTO tagged data using the GVDM Q^2 dependence the number of low-thrust events is about 20% of the total data sample.

Four models have been described above which yield low-thrust events, namely two phase space models, and models for the QCD processes $\gamma\gamma \to q\bar{q}g$ and $\gamma\gamma \to q\bar{q}q\bar{q}$. The cross-sections for these processes are not precisely known; also the cross-section for the VDM is uncertain due to the extrapolation of the PLUTO data [3] from $Q^2 \sim 0.5\,\mathrm{GeV}^2$ to $Q^2 \sim 0.0\,\mathrm{GeV/c}^2$. Consequently we have fitted the data of Fig. 3 to

$$R(p_T^{jet}) = aR_{VDM}(p_T^{jet}) + R_{QPM}(p_T^{jet}) + bR_{multijet}(p_T^{jet})$$

where a and b are parameters that are fitted subject to the constraint that the number of events predicted by the sum of the two-jet and multijet models is equal to the number of data events. R, R_{VDM}, R_{QPM} and $R_{multijet}$ are the $\tilde{R}^{\gamma\gamma}(p_T^{jet})$ distributions of the data, VDM, QPM and multijet models, respectively. The fitted fractions (χ^2) of multijet events are $6 \pm 1\%$ (66), $10 \pm 1\%$ (23), $16 \pm 1\%$ (22) and $26 \pm 2\%$ (7) for the PS1, PS2, $q\bar{q}g$ and $q\bar{q}q\bar{q}$ models respectively. The results of the fits are shown in Fig. 7. The fits show that the PS1 model can be excluded due to the poor χ^2 and that the other models, individually or mixed,

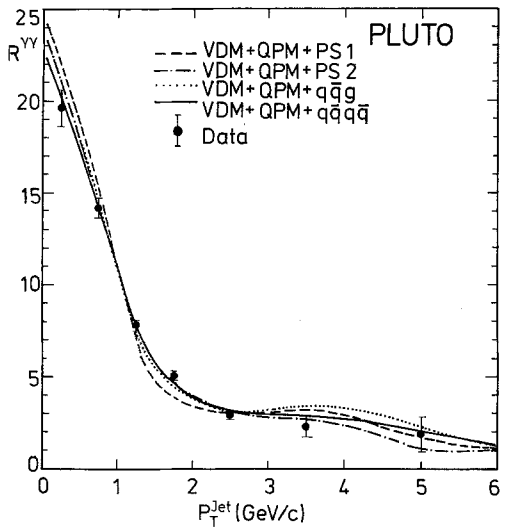

Fig. 7. $\tilde{R}^{\gamma\gamma}$ versus p_T^{jet} for all data. Each curve results from the sum of the two-jet model and a multijet model (see text)

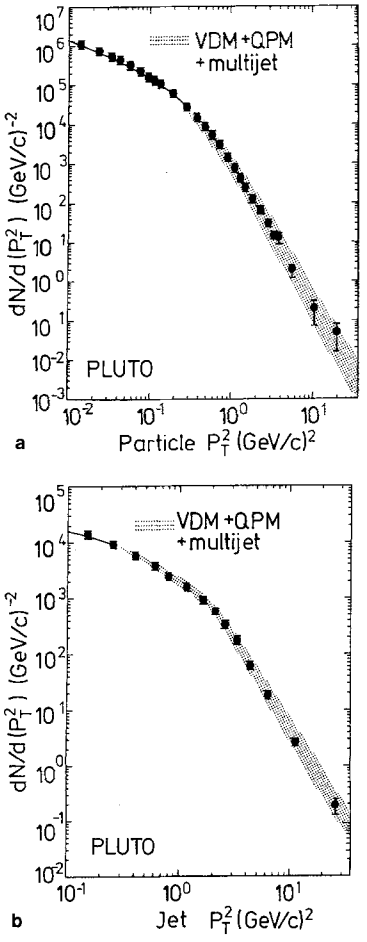

Fig. 8a, b. The charged particle and jet p_T^2 distributions. The p_T of particles and jets are measured with respect to the e^+e^- beam direction in the hadronic CM frame. The shaded area represents the prediction from the sum of the two-jet model and multijet models

would give a satisfactory description of the $\tilde{R}^{\gamma\gamma}(p_T^{\text{jet}})$ distribution*. For the $q\bar{q}g$ and $q\bar{q}q\bar{q}$ models the fraction required is close to the 20% estimated using VDM extrapolated from the PLUTO tagged data. This fraction is in agreement with theoretical expectations [4]. On the basis of the fits, we cannot distinguish between the PS2, $q\bar{q}g$ and $q\bar{q}q\bar{q}$ models. Also the thrust distribution does not allow a distinction. We therefore show in Figs. 5 and 6 the range of predictions of these models as a shaded band. These figures demonstrate that the sum of a multijet model and the two-jet model gives a good description of the thrust distribution, both on average and as a function of p_T^{jet}. The agreement with the data is further demonstrated in Fig. 8 which shows the particle and jet p_t^2 distributions.

Conclusions

The existence of jet production in $\gamma\gamma$ interactions at $Q^2=0$ has been shown. The conclusions of the jet analysis are:

- For high jet transverse momentum, the data approach from above the predictions of a Quark Parton Model with constituent masses and fractionally charged quarks.
- When two-jet events are selected by requiring thrust $\geqq 0.9$, the data at all jet transverse momenta are described well by the incoherent sum of a Vector Dominance derived model and the Quark Parton Model.
- Between 10 and 26% of the events do not have a two-jet topology. These events can be described by models representing multijet processes.

Acknowledgments. We thank the DESY directorate for the hospitality extended to the university groups. We acknowledge the excellent performance of the PETRA machine group and the staff of the DESY computer centre during the experiment. We acknowledge the efforts of all the engineers and technicians who have participated in the construction and maintenance of the apparatus.

References

1. S.J. Brodsky, T.A. DeGrand, J.F. Gunion, J.H. Weis: Phys. Rev. Lett. **41**, 672 (1978)
2. JADE Collab. W. Bartel et al.: Phys. Lett. **107B**, 163 (1981); TASSO Collab. R. Brandelik et al.: Phys. Lett. **107B**, 290 (1981); W. Wagner: Proc. Int. Conf. on High Energy Physics, Madison, Vol. 2, 576 (1986); TASSO Collab. M. Althoff et al.: Phys. Lett. **138B**, 219 (1984); F. Foster: Proc. of the Int. Workshop on Photon-Photon Collisions 69 (1984), reporting on unpublished results of the CELLO collaboration
3. PLUTO Collab. Ch. Berger et al.: Z. Phys. C – Particles and

* Note that the fit errors and χ^2 are based on the statistical errors only

Fields **26**, 191 (1984); PLUTO Collab. Ch. Berger et al.: Z. Phys. C – Particles and Fields **29**, 499 (1985); S.L. Cartwright: Ph. D. thesis, University of Glasgow (1983); A. Tylka: Ph. D. thesis, University of Maryland (1984)
4. S.J. Brodsky, T.A. DeGrand, J.F. Gunion, J.H. Weis: Phys. Rev. **D19**, 1418 (1979); W.J. Stirling: Proceedings of the Fifth International Workshop on $\gamma\gamma$ Collisions, Aachen, pp. 142–174 (1983)
5. L. Criegee, G. Knies: Phys. Rep. **83**, 153 (1982)
6. PLUTO Collab. Ch. Berger et al.: Z. Phys. C – Particles and Fields **26**, 199 (1984)
7. D. Hendry: Ph. D. thesis, University of Glasgow (1985)
8. J.A.M. Vermaseren: Proceedings of the International Workshop on $\gamma\gamma$ Collisons, Amiens 1980. Lect. Notes Phys. **134**. Berlin, Heidelberg, New York: Springer 1980
9. R.P. Feynman, R.D. Field: Nucl. Phys. **B136**, 1 (1978)
10. D. Schlatter: SLAC Report No. SLAC-PUB-2982 (1982)